

## Nonpeptidic Inhibitors of Human Leukocyte Elastase. 2. Design, Synthesis, and *in Vitro* Activity of a Series of 3-Amino-6-arylopyridin-2-one Trifluoromethyl Ketones

James R. Damewood, Jr.,<sup>†</sup> Philip D. Edwards,<sup>†</sup> Scott Feeney,<sup>†</sup> Bruce C. Gomes,<sup>§</sup> Gary B. Steelman,<sup>†</sup> Paul A. Tuthill,<sup>†</sup> Joseph C. Williams,<sup>§</sup> Peter Warner, Sheila A. Woolson,<sup>†</sup> Donald J. Wolanin,<sup>\*,†,‡</sup> and Chris A. Veale<sup>\*,†</sup>

Departments of Medicinal Chemistry and Pharmacology, ZENECA Pharmaceuticals Group, A Business Unit of ZENECA Inc., 1800 Concord Pike, Wilmington, Delaware 19897

Received June 8, 1994<sup>®</sup>

A series of potent nonpeptidic inhibitors of the enzyme human leukocyte elastase (HLE) is reported. These inhibitors contain a 3-amino-2-pyridone ring as a central template in which the pyridone carbonyl and 3-position NH group are thought to form important hydrogen bonding interactions with the Val-216 residue of HLE. Substitution of the 6-position of the pyridone ring by various alkyl and aryl groups was found to afford increases in the *in vitro* potency of these inhibitors. A 6-position phenyl group, compound **10f**, was found to result in a large increase in binding affinity, which was not obtained when the phenyl group was placed in either the 4- or 5-position of the molecule. Compound **10f** was found to have good selectivity for HLE over other proteolytic enzymes, with the exception of bovine pancreatic chymotrypsin (BPC). Substitution of the 6-phenyl group in these molecules was found to decrease binding affinity for BPC without adversely affecting affinity for HLE.

### Introduction

Human leukocyte elastase (HLE) is one of several serine proteases contained in the azurophilic granules of human neutrophils.<sup>1</sup> Upon activation of the neutrophil by inflammatory stimuli, degranulation can occur, releasing these proteases into the extracellular environment. Extracellular HLE is capable of the proteolytic degradation of a broad range of substrates, including the structural proteins elastin and type IV collagen, both of which are components of connective tissues. Normally, the lung is shielded from excessive elastolytic activity by a number of natural proteinaceous inhibitors. These inhibitors include:  $\alpha_1$ -proteinase inhibitor ( $\alpha_1$ -PI), which is present in plasma and guards the lower airways;<sup>2</sup> secretory leukocyte protease inhibitor (SLPI), which is secreted by mucosal cells and is thought to protect the larger airways;<sup>3</sup> and elafin which is found mainly in the skin, but has also recently been detected in bronchial secretions.<sup>4,5</sup> In a number of pathophysiological states, these natural proteinaceous inhibitors ineffectively regulate elastase activity. The resulting unrestrained elastolytic activity is associated with the abnormal tissue turnover found in pulmonary emphysema and in diseases such as cystic fibrosis and chronic bronchitis in which mucus secretion and impaired host defense are major components.<sup>6-9</sup>

Our goal has been to develop inhibitors of HLE that can be used to supplement the natural defenses against elastolytic proteolysis in disease states where endogenous inhibitors ineffectively control elastase activity. Previous reports from these laboratories have disclosed several series of potent, reversible, peptidic inhibitors of HLE that show long-lasting inhibition of elastase activity after intratracheal administration in animal

models.<sup>10,11</sup> One of these, ICI-200,880 (**1**, Figure 1), is currently undergoing clinical evaluation.<sup>12</sup> As a follow-up to ICI-200,880, we sought to discover elastase inhibitors that could be administered by the oral route. Previous papers in this series discuss the preliminary design considerations that led to the development of a novel series of nonpeptidic, trifluoromethyl ketone-containing inhibitors of HLE.<sup>13</sup> These pyridone-based inhibitors (e.g., **2**) are exemplified in Figure 1. In this work we report the extension of this series to compounds that inhibit elastase activity at nanomolar ( $K_i$ ) levels *in vitro*. Future reports will describe the extension of these efforts to include compounds that demonstrate oral activity in animal models.<sup>14,15</sup>

### Design Considerations

Our design of inhibitors such as **2** was based in large part on information obtained from several X-ray crystal structures of peptidic inhibitors bound to HLE and the closely related enzyme, porcine pancreatic elastase (PPE). Bode<sup>16</sup> has reported the crystal structure of the complex between HLE and the third domain of the turkey ovomucoid inhibitor (TOMI). In this complex, the inhibitor occupies an extended binding region ( $S_3'$  to  $S_5$ ) in the active site of the enzyme. The  $P_3$ - $P_1$  residues of this proteinaceous inhibitor form an anti-parallel  $\beta$ -sheet binding arrangement with the Ser-214 to Val-216 section of the enzyme. Several inhibitor-enzyme hydrogen bonds are observed in this binding arrangement. Particularly noteworthy are a pair of hydrogen bonds between the  $P_3$  residue of the inhibitor (Cys-16i) and the Val-216 residue of the enzyme.

In conjunction with our laboratories, Meyer<sup>17-19</sup> has reported the crystal structures of several low molecular weight, reversible peptidic inhibitors bound to PPE. In these structures, an electrophilic carbonyl present in the inhibitor forms a hemiketal linkage with the active site Ser-195 hydroxyl. A schematic representation of the binding interactions found in the complex of Ac-Ala-Pro-

<sup>†</sup> Department of Medicinal Chemistry.

<sup>§</sup> Department of Pharmacology.

<sup>‡</sup> Current address: Miles Pharmaceuticals, West Haven, CT.

<sup>®</sup> Abstract published in *Advance ACS Abstracts*, September 1, 1994.

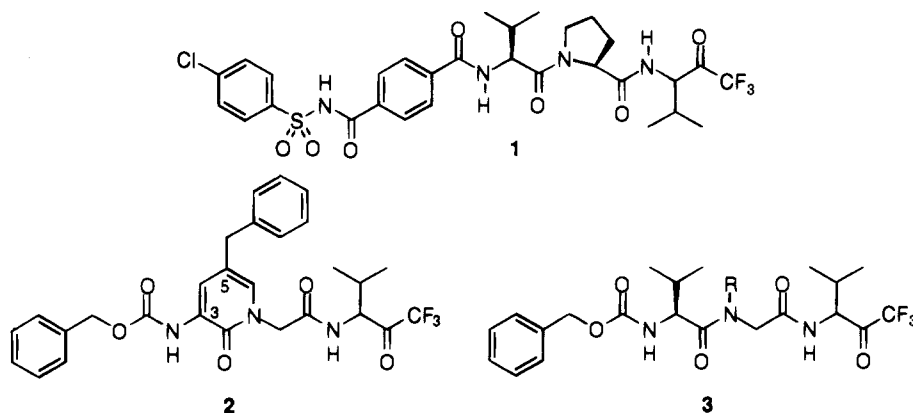


**Figure 1.** Elastase inhibitors (*in vitro* potencies: **1**  $K_i = 0.2$  nM; **2**  $K_i = 40$  nM; **3**  $R = \text{benzyl}$ ,  $K_i = 2.0$  nM).

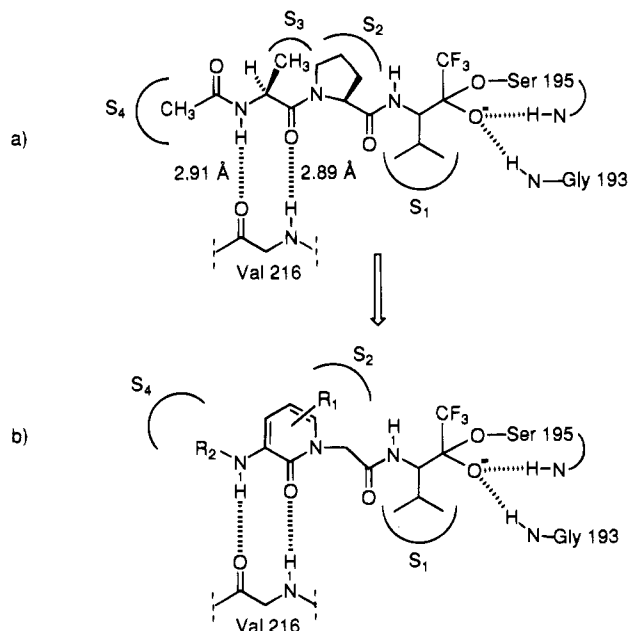


**Figure 2.** (a) A schematic diagram of the binding interactions found in the crystal structure described in ref 17. Hydrogen bond distances shown refer to heteroatom to heteroatom distances. (b) The proposed binding mode of pyridonyl trifluoromethyl ketones in HLE.

Val-trifluoromethyl ketone with PPE, is shown in Figure 2a. As in the HLE-TOMI complex, a pair of hydrogen bonds are found between the  $P_3$  residue (Ala) of the inhibitor and Val-216 of PPE. Closer examination of these, and other crystal structures, revealed additional pieces of structural information that were found to be useful in the design of nonpeptidic inhibitors such as **2**. It was noted that the carbonyl (C=O) and amido (NH) groups of Val-216 in both enzymes are approximately coplanar. A similar, nearly coplanar arrangement was noted for the reciprocal pair of hydrogen bonding partners (NH, C=O) located at  $P_3$  of the peptidic inhibitors. Maintaining this nearly coplanar arrangement in a nonpeptidic inhibitor was viewed as an important design consideration. The  $S_3$  subsite on HLE was observed to consist of a relatively shallow area on the solvent-exposed surface of the enzyme. Therefore, it seemed reasonable to assume that potent nonpeptidic inhibitors would not have to occupy this relatively shallow binding region. This structural suggestion was also consistent with our previous SAR studies for peptide-based inhibitors of HLE, which had revealed a wide variety of hydrophilic residues were tolerated in

the  $P_3$  region of the molecule, as this peptide side chain is directed toward solution.<sup>20</sup>

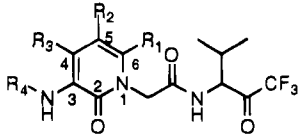
Together, these observations suggested that it might be possible to replace the  $P_3$  residue of the peptidic inhibitors with a planar molecular fragment, such as the pyridone ring of **2**. Molecular mechanics modeling of structures such as **2** into the active site region of HLE demonstrated that the pyridone carbonyl and 3-position NH groups could be positioned so that hydrogen bonding interactions could be formed with Val-216. These modeling studies also suggested that the pyridone nucleus did not access the  $S_2$  subsite of the enzyme. Our previous experience with a series of *N*-alkylglycine-containing trifluoromethyl ketones (e.g., **3**, Figure 1) had demonstrated the importance of placing hydrophobic functionality into the  $S_2$  pocket of HLE in order to improve inhibitor binding affinity.<sup>21</sup> Modeling investigations suggested that placement of hydrophobic groups (e.g., phenyl, benzyl) at the 5- or 6-position of the pyridone ring might result in substituents that were able to reach into the  $S_2$  pocket. These initial modeling efforts were, however, unable to distinguish which of these two positions would be optimal for substitution. Our previous report has detailed the structure-activity relationships of substitution at the 5-position of the pyridone ring.<sup>13b</sup> In this paper we extend descriptions of these efforts to include the 6-position of the molecule.

## Synthetic Chemistry

The compounds described in Table 1 were prepared by the procedures shown in Schemes 1–5.

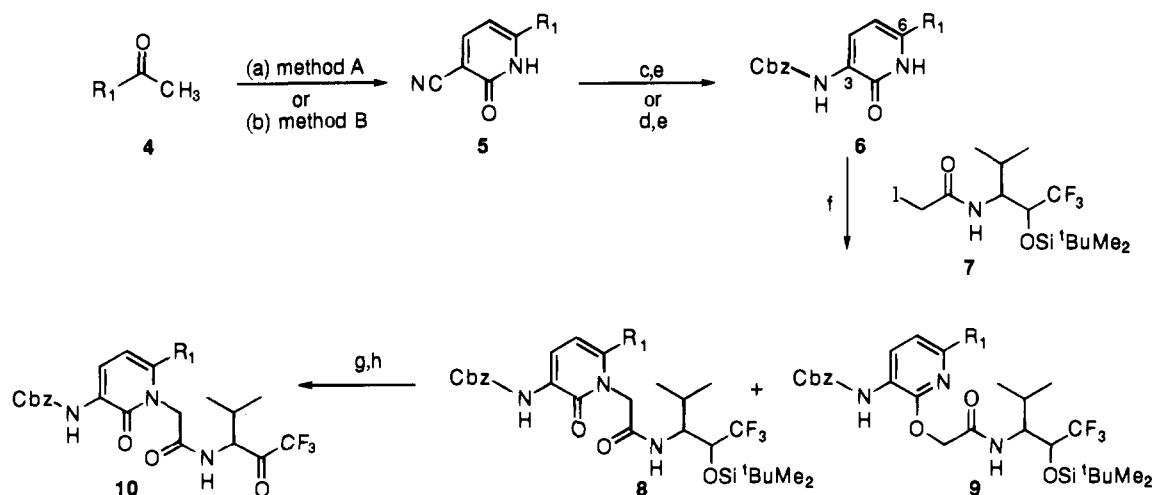
The 6-aryl-substituted pyridones **5** were made from the appropriate acetophenones **4** (Scheme 1) using either general method A or B.<sup>22,23</sup> The pyridone 3-position cyano group in **5** was converted into the benzyloxy-carbonyl-protected amine **6** by a two-step procedure. In the first step, the cyano group was hydrolyzed to the corresponding carboxylic acid by treatment with HBr in acetic acid or by alkaline hydrolysis under vigorous conditions. The second step was the conversion of the acid into the urethane, via the isocyanate, using the modification of the Curtius reaction described by Ni-nomiya et al.<sup>24</sup>

Addition of the pendant trifluoromethyl-containing side chain was accomplished by alkylation of the pyridone ring with iodide **7**.<sup>25</sup> This procedure resulted in mixtures of *N*- and *O*-alkylated products in which the *O*-alkylated isomer generally predominated. For example, alkylation of the 6-phenylpyridone ( $R_1 = \text{Ph}$ )

**Table 1.** Inhibitory Activity against Human Leukocyte Elastase


compd	R <sub>1</sub>	R <sub>2</sub>	R <sub>3</sub>	R <sub>4</sub>	K <sub>i</sub> (nM) HLE <sup>a</sup>	formula	cyclization procedure <sup>b</sup>
<b>2</b>	H	CH <sub>2</sub> Ph	H	Cbz	40 ± 9	C <sub>28</sub> H <sub>28</sub> F <sub>3</sub> N <sub>3</sub> O <sub>5</sub> ·0.75H <sub>2</sub> O	—
<b>10a</b>	H	H	H	Cbz	280 ± 78	C <sub>21</sub> H <sub>22</sub> F <sub>3</sub> N <sub>3</sub> O <sub>5</sub> ·0.33H <sub>2</sub> O	—
<b>10b</b>	CH <sub>3</sub>	H	H	Cbz	360 ± 150	C <sub>22</sub> H <sub>24</sub> F <sub>3</sub> N <sub>3</sub> O <sub>5</sub> ·0.4H <sub>2</sub> O	—
<b>10c</b>	CH <sub>2</sub> Ph	H	H	Cbz	66 ± 12	C <sub>28</sub> H <sub>28</sub> F <sub>3</sub> N <sub>3</sub> O <sub>5</sub> ·0.4H <sub>2</sub> O	—
<b>10d</b>	CH <sub>2</sub> CH <sub>2</sub> Ph	H	H	Cbz	79 ± 10	C <sub>28</sub> H <sub>30</sub> F <sub>3</sub> N <sub>3</sub> O <sub>5</sub>	—
<b>10e</b>	CH=CHPh	H	H	Cbz	33 ± 8	C <sub>29</sub> H <sub>28</sub> F <sub>3</sub> N <sub>3</sub> O <sub>5</sub>	—
<b>10f</b>	Ph	H	H	Cbz	4.5 ± 0.8	C <sub>27</sub> H <sub>26</sub> F <sub>3</sub> N <sub>3</sub> O <sub>5</sub>	A
<b>29</b>	H	H	Ph	Cbz	320 ± 50	C <sub>27</sub> H <sub>26</sub> F <sub>3</sub> N <sub>3</sub> O <sub>5</sub> ·0.25H <sub>2</sub> O	—
<b>31</b>	H	Ph	H	Cbz	300 ± 40	C <sub>27</sub> H <sub>26</sub> F <sub>3</sub> N <sub>3</sub> O <sub>5</sub>	—
<b>10g</b>	4-ClC <sub>6</sub> H <sub>4</sub>	H	H	Cbz	6.6 ± 0.3	C <sub>27</sub> H <sub>26</sub> ClF <sub>3</sub> N <sub>3</sub> O <sub>5</sub>	A
<b>10h</b>	3-ClC <sub>6</sub> H <sub>4</sub>	H	H	Cbz	3.5 ± 0.3	C <sub>27</sub> H <sub>25</sub> ClF <sub>3</sub> N <sub>3</sub> O <sub>5</sub> ·0.2H <sub>2</sub> O	A
<b>10i</b>	2-ClC <sub>6</sub> H <sub>4</sub>	H	H	Cbz	11 ± 1.8	C <sub>27</sub> H <sub>26</sub> ClF <sub>3</sub> N <sub>3</sub> O <sub>5</sub>	A
<b>10j</b>	4-(CH <sub>3</sub> O)C <sub>6</sub> H <sub>4</sub>	H	H	Cbz	8.5 ± 2.4	C <sub>28</sub> H <sub>28</sub> F <sub>3</sub> N <sub>3</sub> O <sub>6</sub>	B
<b>10k</b>	3-( <i>t</i> BuO)C <sub>6</sub> H <sub>4</sub>	H	H	Cbz	4.4 ± 2.6	C <sub>31</sub> H <sub>34</sub> F <sub>3</sub> N <sub>3</sub> O <sub>6</sub> ·0.5H <sub>2</sub> O	A
<b>10l</b>	3-(HO)C <sub>6</sub> H <sub>4</sub>	H	H	Cbz	5.6 ± 0.9	C <sub>27</sub> H <sub>26</sub> F <sub>3</sub> N <sub>3</sub> O <sub>6</sub>	—
<b>10m</b>	3,5-(CH <sub>3</sub> O)C <sub>6</sub> H <sub>3</sub>	H	H	Cbz	3.8 ± 1.5	C <sub>29</sub> H <sub>30</sub> F <sub>3</sub> N <sub>3</sub> O <sub>7</sub>	B
<b>10n</b>	4-(CH <sub>3</sub> )C <sub>6</sub> H <sub>4</sub>	H	H	Cbz	31 ± 4	C <sub>28</sub> H <sub>28</sub> F <sub>3</sub> N <sub>3</sub> O <sub>5</sub>	B
<b>10o</b>	3-Pyridyl	H	H	Cbz	9.1 ± 1.6	C <sub>26</sub> H <sub>26</sub> F <sub>3</sub> N <sub>4</sub> O <sub>5</sub> ·0.25H <sub>2</sub> O	A
<b>10p</b>	4-(CO <sub>2</sub> H)C <sub>6</sub> H <sub>4</sub>	H	H	Cbz	42 ± 15	C <sub>28</sub> H <sub>26</sub> F <sub>3</sub> N <sub>3</sub> O <sub>7</sub>	—
<b>10q</b>	3-(CO <sub>2</sub> H)C <sub>6</sub> H <sub>4</sub>	H	H	Cbz	32 ± 5	C <sub>28</sub> H <sub>26</sub> F <sub>3</sub> N <sub>3</sub> O <sub>7</sub> ·0.5H <sub>2</sub> O	—

<sup>a</sup> Method reported in ref 12. <sup>b</sup> Refers to the cyclization procedure (method A or method B) described in Scheme 1.

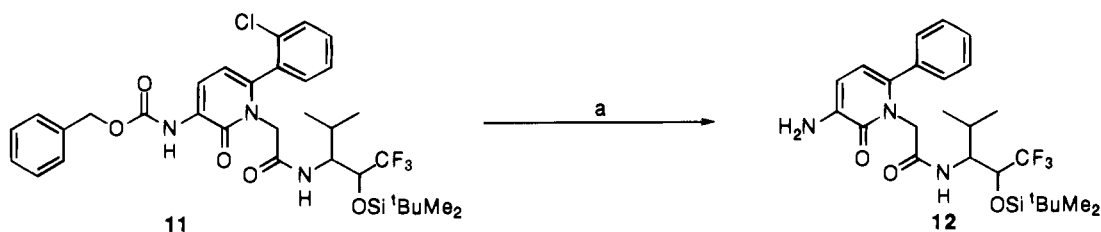
**Scheme 1<sup>a</sup>**

<sup>a</sup> Generic group R<sub>1</sub> is defined in Table 1. Reagents: (a) (method A) (i) (CH<sub>3</sub>)<sub>2</sub>NCH(OCH<sub>3</sub>)<sub>2</sub>, CH<sub>3</sub>CN; (ii) cyanoacetamide, CH<sub>3</sub>ONa, DMF; (b) (method B) (i) EtOC(O)H, CH<sub>3</sub>ONa, THF; (ii) cyanoacetamide, acetic acid, H<sub>2</sub>O; (c) 48% HBr/acetic acid; (d) 50% NaOH, sealed bomb, 140 °C; (e) DPPA, Et<sub>3</sub>N, dioxane, then benzyl alcohol; (f) NaH, **7**, DMF; (g) TBAF, THF; (h) EDC, Cl<sub>2</sub>CHCO<sub>2</sub>H, toluene, DMSO.

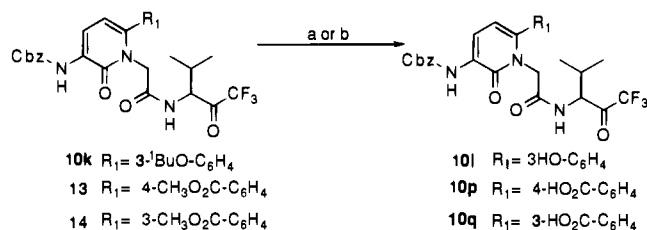
with iodide **7** was found to produce a 1:2.4 ratio of the desired nitrogen-alkylated product **8** to the unwanted oxygen-alkylated product **9**. In an attempt to overcome the poor regioselectivity obtained in the alkylation reaction, a number of different bases, solvents, and modifications in reaction conditions were explored, but none successfully increased the ratio of nitrogen-alkylated product. In the course of probing the effect of substitution of the pyridone 6-position on biological activity, we found that the ratio of N- to O-alkylated isomers could be reversed to favor the N-alkylated pyridone by placement of a chlorine atom in the ortho position of the 6-aryl substituent. This variation resulted in a 5 to 1 ratio in favor of the desired nitrogen-substituted pyridone. The *o*-chlorophenyl compound has been found to be synthetically useful for the preparation of 6-phenylpyridones, as the chlorine atom can subsequently be removed via hydrogenolysis, pro-

viding a key intermediate (**12**) for variation of the substituent on the pyridone-3-amino group (Scheme 2).<sup>26</sup> Removal of the *tert*-butyldimethylsilyl protecting group in **8** (Scheme 1) followed by oxidation of the resulting trifluoromethyl alcohol using a modified Pfitzner–Moffatt<sup>27</sup> oxidation provided the desired trifluoromethyl ketones **10**. The phenol **10l** and carboxylic acids **10p** and **10q** were then made from the corresponding *tert*-butyl ether (**10k**) or methyl esters (**13** and **14**), respectively, as shown in Scheme 3.

Pyridones containing 6-alkyl substituents were synthesized by the method shown in Scheme 4. The desired 6-alkyl substituents were incorporated either as part of the pyridone ring-forming process (e.g., **16** and **17**) or by alkylation of the dianion of 6-methyl-3-cyanopyridone<sup>28</sup> (**16**) with the indicated electrophile to yield **18** or **19**.<sup>29</sup> The intermediate pyridonecarboxylic acids were obtained by treatment of the cyano compounds with HBr

Scheme 2<sup>a</sup>

<sup>a</sup> Reagents: (a) 10%Pd/C, H<sub>2</sub>, sodium methoxide, methanol.

Scheme 3<sup>a</sup>

<sup>a</sup> Reagents: (a) (10k to 10l) TFA, CH<sub>2</sub>Cl<sub>2</sub>; (b) LiOH·H<sub>2</sub>O, THF, H<sub>2</sub>O.

in acetic acid, which in the case of the benzaldehyde adduct **18** also effected dehydration of the benzylic alcohol to give the *trans*-olefin. The resulting carboxylic acids were then transformed into the protected amines **20–23** using diphenylphosphoryl azide (Aldrich) and benzyl alcohol.

In contrast to the problems encountered in the alkylation of 6-aryl-substituted pyridones, alkylation of the 6-alkyl-substituted pyridones using either iodide **7** or *tert*-butyl bromoacetate was found to give predominately the *N*-alkylated isomers. Deprotection of the *tert*-butyl ester was achieved using trifluoroacetic acid to give acids **24–27**. Carbodiimide-mediated coupling of these acids with 3-amino-1,1,1-trifluoro-4-methyl-2-pentanol<sup>10</sup> furnished the penultimate trifluoromethyl alcohols, which were then oxidized to the corresponding trifluoromethyl ketones **10b–e**.

The synthesis of pyridones that contain phenyl substituents in the 4- or 5-positions is described in Scheme 5. The 4-phenylpyridone **28** was obtained by the condensation of acetophenone with cyanoacetamide followed by treatment with *N,N*-dimethylformamide dimethyl acetal in refluxing DMF. Compound **28** was then converted to **29** using the methodology described in Scheme 1. The 5-phenylpyridone (**31**) was prepared by a palladium-mediated coupling of phenylboric acid with the 5-iodopyridone **30** and subsequent deprotection and oxidation to furnish **31**.<sup>13,30</sup>

## Biological Results

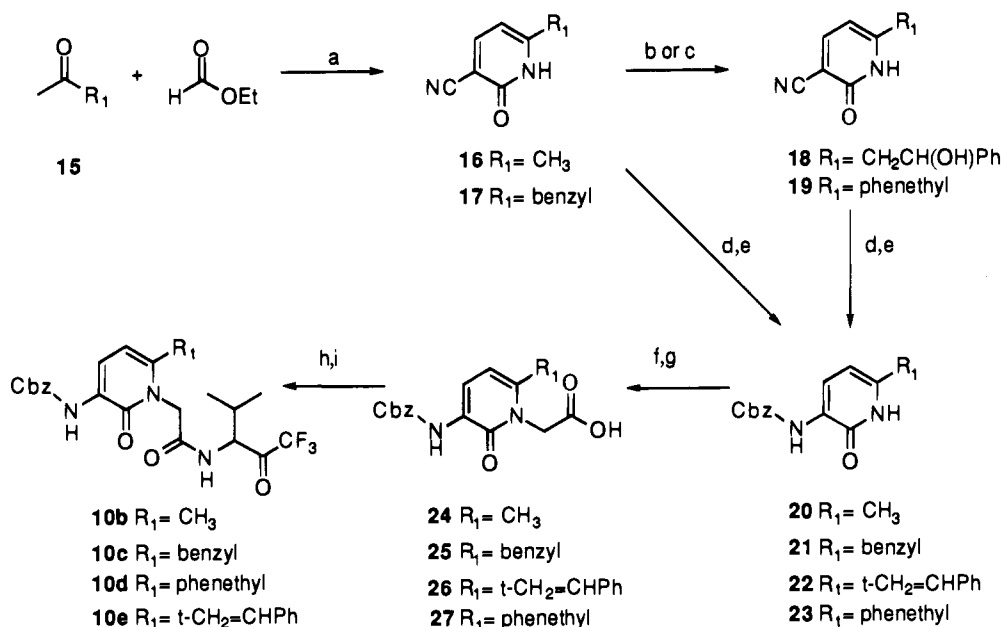
The *in vitro* activity of the compounds in Table 1 was measured by their ability to inhibit the elastase-mediated hydrolysis of the synthetic substrate MeO-Suc-Ala-Ala-Pro-Val-pNA.<sup>12</sup>

Initially, we prepared a series of compounds that contained substituents of increasing size and lipophilicity in the 6-position of the pyridone ring. Methyl substitution (**10b**) was found to offer no advantage in binding affinity over the unsubstituted compound **10a**. Larger and more lipophilic substituents, such as those present in **10c–e**, improved affinity by 3–8-fold. Benzyl substitution at either C-5 or C-6 (compare **2** and **10c**) resulted in inhibitors of similar potency. However, a

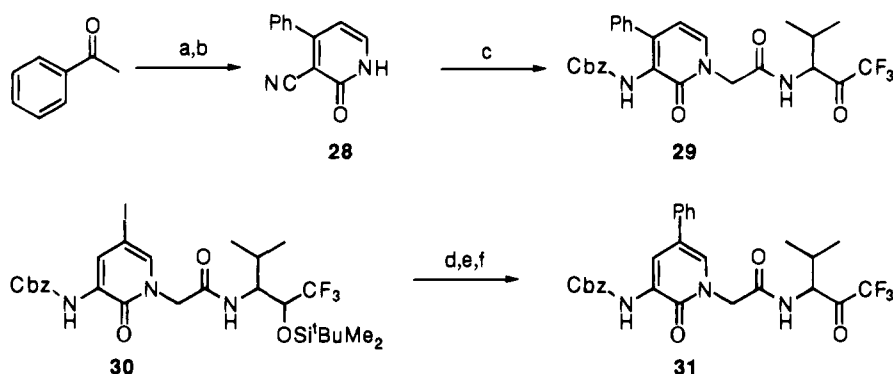
6-position phenyl substituent (**10f**) showed a dramatic increase in affinity (>60-fold relative to **10a**), resulting in nanomolar (*K<sub>i</sub>*) inhibition of HLE. Similar increases in potency were *not* observed, however, when a phenyl group was placed in either the 4- or 5- (compounds **29** and **31**) position.

The observation that 6-position substituents with different geometric features (e.g., 6-benzyl) but similar lipophilicity did not result in similar increases in binding affinity suggested that geometrically specific hydrophobic binding interactions between the phenyl substituent and HLE may be involved.<sup>31</sup> In addition, 6-position substituents could serve to restrict the conformational space available to the neighboring pyridone 1-position substituent, maintaining that group in an optimal conformation for interaction with HLE. In this regard, a conformationally constrained phenyl substituent might be more effective than the more flexible benzyl which could, conceptually, escape major steric interactions with the 1-position side chain. To investigate these possibilities further, aqueous molecular dynamics (MD) and free energy perturbation (FEP) simulations for **10f** and **10a** were performed for both the solution state and with the inhibitors complexed to HLE.<sup>32</sup>

Aqueous MD simulation of **10f** in HLE shows that many of the important inhibitor–enzyme interactions observed in peptide based inhibitors are maintained for this pyridone derivative (see Figure 2). The oxyanion formed from the carbonyl oxygen of the trifluoromethyl ketone hydrogen bonds to the backbone NH groups of Gly-193 and Ser-195. The desired hydrogen bonding interactions between the pyridone ring carbonyl oxygen and 3-position amine NH with the backbone NH and carbonyl oxygen of Val-216 are maintained throughout the simulation. The 6-phenyl substituent nestles into the S<sub>2</sub> pocket defined by Leu-99, Phe-215, and His-57. Figure 3 shows one time point from the MD simulations that demonstrates the interaction between the S<sub>2</sub> pocket and the 6-phenyl group. FEP simulations were employed to investigate the free energy cost of removing the 6-phenyl substituent from the pyridone nucleus. The Δ*G* value of 1.76 ± 0.6 kcal/mol obtained for this process corresponds to a *K<sub>i</sub>* ratio of approximately 20 in favor of the substituted inhibitor. The reasonable agreement of this value with the experimentally determined *K<sub>i</sub>* ratio (60-fold difference between **10f** and **10a**) suggested that the proposed pyridone binding mode was, indeed, consistent with the experimental data. To investigate the possible effects of the 6-phenyl substituent on the conformation of the N-1 side chain, 100PS aqueous MD simulations were performed for **10a** and **10f**. For both of these compounds, the orientations of the N-1 side chains were very similar, forming average torsion angles

Scheme 4<sup>a</sup>

<sup>a</sup> Reagents: (a) (i)  $\text{NaOCH}_3$ ,  $\text{Et}_2\text{O}$ ; (ii) cyanoacetamide, piperidine acetate,  $\text{H}_2\text{O}$ ; (b) (**16** to **18**) LDA, THF, then benzaldehyde; (c) (**16**–**19**) LDA, THF, then benzyl bromide; (d) 48% HBr, acetic acid; (e) DPPA,  $\text{Et}_3\text{N}$ , dioxane, then benzyl alcohol; (f) NaH, DMF, then *tert*-butyl bromoacetate; (g) TFA,  $\text{CH}_2\text{Cl}_2$ ; (h) EDC, DMAP, 3-amino-1,1,1-trifluoro-4-methyl-2-pentanol hydrochloride, DMF; (i) EDC,  $\text{Cl}_2\text{CHCO}_2\text{H}$ , toluene, DMSO.

Scheme 5<sup>a</sup>

<sup>a</sup> Reagents: (a) cyanoacetamide,  $\text{NH}_4\text{OAc}$ , AcOH, toluene; (b) *N,N*-dimethylformamide dimethyl acetal, DMF; (c) steps d–h in Scheme 1; (d) phenylboric acid, tetrakis(triphenylphosphine)palladium(0),  $\text{Na}_2\text{CO}_3$ , THF, ethanol,  $\text{H}_2\text{O}$ ; (e) TBAF, THF; (f) EDC,  $\text{Cl}_2\text{CHCO}_2\text{H}$ , toluene, DMSO.

with the pyridone ring of  $103^\circ$  and  $98^\circ$ , respectively. Thus, **10a** and **10f** adopt similar conformations in solution on time average. Indeed, even when a near-eclipsed orientation of the N-1 side chain was used as a starting geometry for the aqueous MD simulations for **10a**, the same average orientation was ultimately observed for the molecule. We conclude from these simulations, together with the structure–activity information presented above, that the main role of the 6-phenyl substituent is the formation of favorable hydrophobic interactions with the  $\text{S}_2$  subsite of HLE. No evidence exists for a significant difference in the Boltzmann population of N-1 side chain conformations as a result of 6-phenyl substitution of the pyridone nucleus at physiologically relevant temperatures.

Having found that a 6-phenyl group provided a very favorable effect on inhibitor binding affinity, we sharpened the focus of our SAR investigations to examine a number of 6-position aryl-containing substituents.<sup>33</sup> This work showed that a number of aryl groups were tolerated in the 6-position providing nanomolar or near nanomolar inhibition of HLE (Table 1).

Further examination of the HLE–TOMI crystal structure showed a tyrosine residue (Tyr-94) to be located in the back of the  $\text{S}_2$  pocket, suggesting that 6-aryl substituents containing a hydrogen bond acceptor in the meta position of the aromatic ring might further increase inhibitor potency. To test this idea, we synthesized compounds **10o** and **10q**. Instead of the anticipated increase in affinity, the pyridyl compound lost 2-fold and the *m*-carboxy compound lost 7-fold in potency. Moving the carboxylate to the para position (**10p**) resulted in a somewhat larger decrease in affinity. Combined, these results support the hypothesis that binding in the  $\text{S}_2$  pocket of the enzyme is predominantly hydrophobic in nature and addition of hydrophilic functionality to the pyridone 6-position is inimical to inhibitor potency.

## Enzyme Selectivity

Compound **10f** was selected as a prototypic compound to assess the selectivity of these inhibitors for HLE compared to other enzymes. The affinity of **10f** was measured for a number of other proteases and esterases

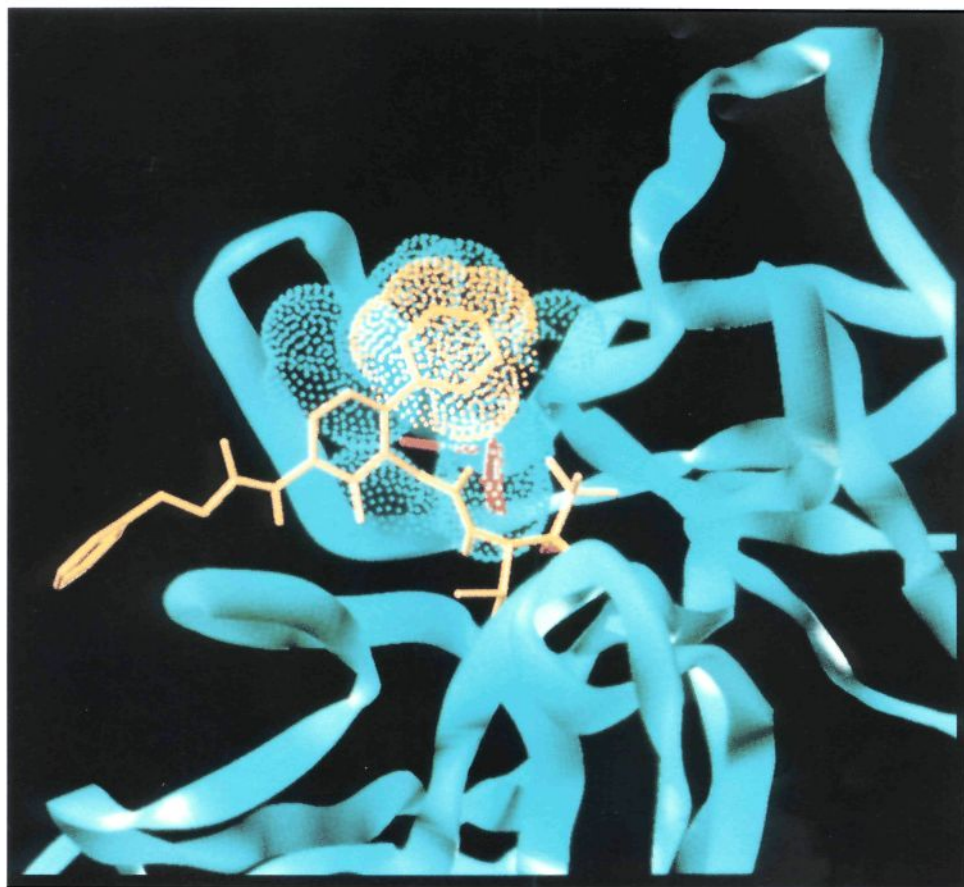


**Figure 3.** Frame from an aqueous molecular dynamics simulation of compound **10f**. Water molecules have been removed for clarity. HLE is shown as a cyan ribbon structure. The catalytic triad (Ser-195, His-57, Asp-102) is shown in red, and **10f** in yellow. A van der Waals surface has been added to the residues that make up the  $S_2$  pocket of HLE (cyan), and the 6-phenyl of **10f** (yellow).

**Table 2.** Enzyme Selectivity Data for Compound **10f**

	$K_i$ (nM)
human leukocyte elastase	$4.5 \pm 0.8$
porcine pancreatic elastase	$4600 \pm 690$
bovine pancreatic chymotrypsin	$55 \pm 10$
bovine pancreatic trypsin	$4800 \pm 5700$
human plasma thrombin	NI ( $26 \mu\text{M}$ ) <sup>a</sup>
papain	$7000 \pm 860$
angiotensin converting enzyme	NI ( $26 \mu\text{M}$ ) <sup>a</sup>
acetylcholinesterase	NI ( $26 \mu\text{M}$ ) <sup>a</sup>
human cathepsin G	NI ( $26 \mu\text{M}$ ) <sup>a</sup>

<sup>a</sup> NI = no inhibition at highest concentration (in parentheses) tested.

of both human and nonhuman origin (Table 2). In general, **10f** showed little or no affinity for other enzymes tested, with the exception of bovine pancreatic chymotrypsin (BPC). Against this enzyme the selectivity ratio ( $K_i$  BPC/ $K_i$  HLE) was found to be 12. Since BPC may be representative of related human proteases, an improvement in this selectivity profile was desired. We therefore investigated a number of 6-substituted compounds against BPC (Table 3) in an attempt to improve specificity. While we found that substitution of the 6-phenyl ring generally had little effect on inhibitor affinity for HLE, affinity for BPC was much more sensitive to this substitution. For example, placement of a chlorine atom in the para position of the phenyl ring (**10g**) resulted in little change in the  $K_i$  for HLE but almost a 10-fold decrease in affinity for BPC. Other 6-position substituents, such as benzyl and phen-

**Table 3.** Enzyme Selectivity Ratios

compd	R	$K_i$ (nM)		ratio chymotrypsin/ HLE <sup>a</sup>
		HLE	chymotrypsin	
<b>10n</b>	4-CH <sub>3</sub> C <sub>6</sub> H <sub>4</sub>	$31 \pm 4$	$720 \pm 163$	23
<b>10g</b>	4-ClC <sub>6</sub> H <sub>4</sub>	$6.6 \pm 0.3$	$500 \pm 180$	76
<b>10f</b>	phenyl	$4.5 \pm 0.8$	$55 \pm 13$	12
<b>2</b>	benzyl	$66 \pm 12$	$6200 \pm 60$	79
<b>10d</b>	phenethyl	$70 \pm 10$	$9600 \pm 1520$	122
<b>10e</b>	CH <sub>2</sub> =CHPh	$33 \pm 8$	$5800 \pm 500$	175
<b>10a</b>	H	$280 \pm 78$	$330000 \pm 10^5$	1031

<sup>a</sup> Refers to the ratio of the  $K_i$  for chymotrypsin to that of the  $K_i$  for HLE.

ethyl, further decreased BPC affinity, but with a concomitant decrease in HLE affinity. Subsequent work in the 6-phenylpyridone series revealed that BPC/HLE selectivity ratios of 3700 could be obtained by incorporation of substituents other than Cbz at the 3-position amino group.<sup>14</sup>

### In Vivo Activity

*In vivo* testing of the compounds in Table 1 was done using a hamster-based acute lung injury model.<sup>12</sup> This model measures the ability of a 37 mg/kg oral dose of inhibitor to protect lung tissue from hemorrhage caused

by a 100  $\mu\text{g}$  challenge of HLE given intratracheally. Unfortunately, upon po administration, none of the compounds in Table 1 gave significant protection of the lung from the elastase-mediated hemorrhage. The lack of oral activity of these compounds is thought to be related to inappropriate physicochemical parameters.<sup>14</sup>

## Summary

This work has demonstrated that it is possible to achieve nanomolar inhibition ( $K_i$ ) of HLE activity in a novel series of nonpeptidic elastase inhibitors. A major contribution to the high levels of affinity for HLE found for these compounds results from specific hydrophobic interactions between the pyridone 6-position phenyl and the  $S_2$  binding pocket of the enzyme. The following paper in this series details the modifications made in these compounds that successfully led to orally active inhibitors.

## Experimental Section

**General Methods.** Analytical samples were homogeneous by TLC and afforded spectroscopic results consistent with the assigned structures. Proton NMR spectra were obtained using either a Bruker WM-250 or AM-300 spectrometer. Chemical shifts are reported in parts per million relative to  $\text{Me}_4\text{Si}$  as internal standard. Mass spectra (MS) were recorded on a Kratos MS-80 instrument operating in the chemical ionization (CI) mode. Elemental analyses for carbon, hydrogen, and nitrogen were determined by the ZENEGA Pharmaceuticals Analytical Department on a Perkin-Elmer 241 elemental analyzer and are within  $\pm 0.4\%$  of theory for the formulas given. Analytical thin-layer chromatography (TLC) was performed on precoated silica gel plates (60F-254, 0.2 mm thick, E. Merck). Visualization of the plates was accomplished by using UV light or phosphomolybdic acid/ethanol charring procedures. Chromatography refers to flash chromatography conducted on Kieselgel 60 230–400 mesh (E. Merck, Darmstadt) using the indicated solvents. Solvents used for reactions or chromatography were either reagent grade or HPLC grade. Reactions were run under an argon atmosphere at ambient temperature unless otherwise noted. Solutions were evaporated under reduced pressure on a rotary evaporator. The following abbreviations are used: THF, tetrahydrofuran; DMF, *N,N*-dimethylformamide; DMSO, dimethyl sulfoxide; EDC, 1-[3-(dimethylamino)propyl]-3-ethylcarbodiimide hydrochloride; TFA, trifluoroacetic acid; DPPA, diphenyl phosphorazide (diphenylphosphoryl azide, Aldrich); Suc, succinyl; pNA, *p*-nitroaniline.

**6-Phenylpyrid-2-one-3-carbonitrile (5,  $R_1 = \text{Ph}$ ) (Method A).** A solution of acetophenone (30.6 g, 255 mmol) and *N,N*-dimethylformamide dimethyl acetal (100 g, 840 mmol) in acetonitrile (500 mL) was heated at reflux for 12 h. The reaction mixture was cooled, the solvent was evaporated, and the resulting yellow semisolid was dried under vacuum. This material was dissolved in DMF (400 mL), to this was added cyanoacetamide (19.4 g, 231 mmol) and sodium methoxide (27.18 g, 500 mmol), and the resulting solution was heated at 100  $^\circ\text{C}$  for 5 h. The reaction was cooled to room temperature and quenched by addition of water (1.2 L), and the solution was made acidic to pH 5 with 10% hydrochloric acid. The resulting yellow precipitate was filtered and dried under vacuum to give the title compound as a yellow solid (35.28 g, 78%):  $^1\text{H NMR}$  (DMSO, 300 MHz)  $\delta$  6.77 (bd, 1H), 7.55 (m, 3H), 7.80 (m, 2H), 8.20 (dd, 1H); MS (CI)  $m/z$  197 ( $M + 1$ ). Anal. ( $\text{C}_{12}\text{H}_9\text{N}_2\text{O}$ ) C, H, N.

**3-[(Benzyloxycarbonyl)amino]-6-phenylpyrid-2-one (6,  $R_1 = \text{Ph}$ ).** A suspension of **5** (15 g, 76 mmol) in a mixture of glacial acetic acid (110 mL) and 48% aqueous hydrobromic acid (50 mL) was heated at reflux for 12 h. The reaction mixture was cooled and diluted with water (50 mL), and the pH was adjusted to 5 with 10% NaOH. The resulting precipitate was filtered, washed successively with 10% hydrochloric acid and

water, and dried under vacuum to give the carboxylic acid as a white solid (14.1 g, 86%). A portion of the carboxylic acid (10 g, 46.5 mmol) was dissolved in dry dioxane (260 mL), and to this was added triethylamine (7.8 mL, 56 mmol) followed by DPPA (11.1 mL, 51 mmol). The solution was heated at reflux for 4 h, and then benzyl alcohol (9.58 mL, 92 mmol) was added followed by heating at reflux for 12 h. The mixture was cooled and the solvent evaporated. The resulting solid was washed successively with 10% hydrochloric acid, saturated sodium bicarbonate, and water. The resulting material was recrystallized from chloroform/methanol (1:2) to provide **6** (4.75 g, 32%):  $^1\text{H NMR}$  (DMSO, 300 MHz)  $\delta$  5.19 (s, 2H), 6.61 (d, 1H), 7.33–7.49 (m, 8H), 7.70 (m, 2H), 7.93 (d, 1H), 8.47 (s, 1H).

**2-[3-[(Benzyloxycarbonyl)amino]-2-oxo-6-phenyl-1,2-dihydro-1-pyridyl]-*N*-[2-[(*tert*-butyldimethylsilyloxy]-3,3,3-trifluoro-1-isopropylpropyl)acetamide (8,  $R_1 = \text{Ph}$ ).** To a solution of **6** (1.7 g, 5.3 mmol) in DMF (50 mL) was added NaH (0.14 g, 5.8 mmol) and the mixture stirred at room temperature for 15 min. To this was added **7** (2.65 g, 5.8 mmol) and the mixture stirred for 12 h. The reaction was quenched by addition of 10% hydrochloric acid and the product extracted into ethyl acetate. The organic solution was washed with 10% hydrochloric acid and water and dried ( $\text{MgSO}_4$ ), and the solvent was evaporated. The resulting material was purified by chromatography (gradient elution, ethyl acetate in dichloromethane, 1:99 to 4:99) to provide **8** (0.97 g, 28%): TLC  $R_f = 0.35$  (dichloromethane:ethyl acetate, 97:3);  $^1\text{H NMR}$  (DMSO, 300 MHz)  $\delta$  0.08 (s, 3H), 0.10 (s, 3H), 0.81 (d, 3H), 0.86 (s, 9H), 0.93 (d, 3H), 1.67–1.78 (m, 1H), 3.81 (t, 1H), 4.22–4.40 (m, 2H), 4.64 (bd, 1H), 5.19 (s, 2H), 6.22 (d, 1H), 7.33–7.48 (m, 10H), 7.63 (d, 1H), 7.92 (d, 1H), 8.53 (s, 1H). Also obtained was the oxygen-alkylated product **9** (2.11 g, 62%): TLC  $R_f = 0.61$  (dichloromethane:ethyl acetate, 97:3);  $^1\text{H NMR}$  (DMSO, 300 MHz)  $\delta$  0.01 (s, 3H), 0.07 (s, 3H), 0.75 (s, 9H), 0.77 (d, 3H), 0.89 (d, 3H), 1.67–1.81 (m, 1H), 3.84 (t, 1H), 4.26 (m, 1H), 4.81 (d, 1H), 5.14 (d, 1H), 5.20 (s, 2H), 7.35–7.48 (m, 9H), 7.62 (d, 1H), 7.99 (dd, 2H), 8.12 (d, 1H), 9.31 (s, 1H); MS (CI)  $m/z$  646 ( $M + 1$ ).

***N*-[2-[(*tert*-Butyldimethylsilyloxy]-3,3,3-trifluoro-1-isopropylpropyl)-2-iodoacetamide (7).** To a solution of 3-amino-1,1,1-trifluoro-4-methyl-2-pentanol hydrochloride<sup>10</sup> (20 g, 96 mmol) and 4-methylmorpholine (21.8 mL, 198 mmol) in THF (480 mL) was added a solution of chloroacetyl chloride (7.7 mL, 97 mmol) in THF (40 mL) and the resulting mixture stirred for 12 h. The mixture was diluted with ethyl acetate, filtered free of solids, and washed with 10% hydrochloric acid, water, saturated aqueous sodium bicarbonate, and brine. The solution was dried ( $\text{MgSO}_4$ ), and the solvent was removed to give the amide as an oil (23.8 g). This oil was dissolved in dichloromethane (96 mL) and cooled in an ice bath, and to this solution was added 2,6-lutidine (22.5 mL, 193 mmol) and then *tert*-butyldimethylsilyl triflate (33 mL, 144 mmol). After being stirred for 12 h the reaction mixture was diluted with ethyl acetate, washed with 10% hydrochloric acid, saturated sodium bicarbonate, and brine, and dried ( $\text{MgSO}_4$ ), and the solvent was removed. The resulting material was chromatographed (gradient elution, hexane:ethyl acetate, 100:0 to 80:20) to provide the pure silyl ether (20.5 g). A portion of this material (15.5 g, 43 mmol) was dissolved in acetone (130 mL), to this was added NaI (19.3 g, 128 mmol), and the mixture was stirred at room temperature for 12 h. The mixture was diluted with water (180 mL), and the resulting precipitate was washed with saturated aqueous sodium thiosulfate and water. The solid was dried under vacuum and then purified by chromatography (gradient elution, hexane:ethyl acetate, 80:20 to 50:50) to provide pure **7** (17.9 g, 92%): TLC  $R_f = 0.30$  (hexane:ethyl acetate, 9:1);  $^1\text{H NMR}$  (DMSO, 300 MHz)  $\delta$  0.17 (s, 3H), 0.18 (s, 3H), 0.96 (d, 3H), 0.98 (s, 3H), 1.01 (s, 9H), 1.75 (m, 1H), 3.75 (s, 2H), 3.92 (t, 1H), 4.15 (q, 1H), 6.50 (d, 1H); MS (CI)  $m/z$  454 ( $M + 1$  for  $^{35}\text{Cl}$ ).

**2-[3-[(Benzyloxycarbonyl)amino]-2-oxo-6-phenyl-1,2-dihydro-1-pyridyl]-*N*-(3,3,3-trifluoro-1-isopropyl-2-oxopropyl)acetamide (10  $R_1 = \text{Ph}$ ).** To a solution of **8** (0.96 g, 1.5 mmol) in THF (8 mL) was added tetrabutylammonium fluoride (1.62 mL, 1.62 mmol) and the mixture stirred for 4.5

h. The reaction mixture was diluted with ethyl acetate and washed with water and brine. The solution was dried (MgSO<sub>4</sub>) and the solvent removed to give the corresponding intermediate trifluoromethyl alcohol as a white solid (0.79 g). The alcohol was dissolved in DMSO (4 mL) and toluene (4 mL) and was treated with EDC (2.81 g, 14.6 mmol) and then dichloroacetic acid (0.48 mL, 5.8 mmol). The resulting solution was allowed to stir for 12 h. The reaction mixture was diluted with ethyl acetate and was washed successively with 10% hydrochloric acid, saturated sodium bicarbonate, and brine. The solution was dried (MgSO<sub>4</sub>) and the solvent removed. The resulting material was purified by chromatography (dichloromethane:ethyl acetate, 95:5) to provide pure **10** (0.53 g, 67%) as a white solid: <sup>1</sup>H NMR (DMSO, 300 MHz) δ 0.83 (d, 3H), 0.89 (d, 3H), 2.10–2.21 (m, 1H), 4.46 (d, 1H), 4.54 (d, 1H), 4.63 (t, 1H), 5.19 (s, 2H), 6.23 (d, 1H), 7.33–7.49 (m, 10H), 7.92 (d, 1H), 8.55 (s, 1H), 8.74 (d, 1H); MS (CI) *m/z* 530 (M + 1). Anal. (C<sub>27</sub>H<sub>26</sub>F<sub>3</sub>N<sub>3</sub>O<sub>5</sub>) C, H, N.

**6-(4-Methoxyphenyl)pyrid-2-one-3-carbonitrile (5, R<sub>1</sub> = 4-CH<sub>3</sub>OC<sub>6</sub>H<sub>4</sub>) (Method B).** To a stirred mixture of sodium methoxide (8.95 g, 165 mmol), ethyl formate (11.55 g, 156 mmol) in THF (60 mL), and ether (60 mL) was added a solution of 4-methoxyacetophenone (10.1 g, 67 mmol) in THF (90 mL) over 0.5 h. After the addition was complete, the addition funnel was replaced with a reflux condenser and the mixture heated at 40 °C for 3 h. The condenser was replaced with a distillation head and the mixture heated at 90 °C until the solvents were removed. The residue was dissolved in water (240 mL), and acetic acid was added to adjust the pH to 9. Cyanoacetamide (10.1 g, 120 mmol) was added and the mixture heated at 90 °C for 18 h. The solvents were decanted to leave a gummy residue, which was washed with 10% hydrochloric acid and then chloroform to give a solid which was filtered, washed with ether, and dried to give **5** (R<sub>1</sub> = 4-CH<sub>3</sub>OC<sub>6</sub>H<sub>4</sub>) (2.97 g, 20%): TLC *R<sub>f</sub>* = 0.5 (methanol:dichloromethane, 4:96); <sup>1</sup>H NMR (DMSO, 250 MHz) δ 3.83 (s, 3H), 6.72 (bs, 1H), 7.10 (d, 2H), 7.79 (d, 2H), 8.16 (d, 1H), 12.62 (bs, 1H); MS (CI) *m/z* 227 (M + 1).

**6-(4-Methoxyphenyl)pyrid-2-one-3-carboxylic Acid (Step d, Scheme 1, R<sub>1</sub> = 4-CH<sub>3</sub>OC<sub>6</sub>H<sub>4</sub>).** A suspension of **5** (R<sub>1</sub> = 4-CH<sub>3</sub>OC<sub>6</sub>H<sub>4</sub>) (2.95 g, 13 mmol) in 50% NaOH (w/w, 13 mL) was heated at 140 °C for 12 h in a sealed pressure vessel. The reaction mixture was cooled to room temperature, diluted with water, and adjusted to pH 1 with concentrated hydrochloric acid. The resulting solids were washed with water and dried under vacuum to provide pure carboxylic acid (3.22 g, 100%): <sup>1</sup>H NMR (DMSO, 300 MHz) δ 3.85 (s, 3H), 6.97 (d, 1H), 7.00 (d, 2H), 7.88 (d, 2H), 8.35 (d, 1H); MS (CI) *m/z* 246 (M + 1).

**2-(3-Amino-2-oxo-6-phenyl-1,2-dihydro-1-pyridyl)-N-[(*tert*-butyldimethylsilyloxy)-3,3,3-trifluoro-1-isopropyl]acetamide (12).** To a solution of **11** (100 g, 0.147 mol) in ethanol (1.2 L) was added palladium on carbon (10% w/w) and the mixture shaken under a hydrogen atmosphere (3.4 bar) for 6 h. The hydrogen was removed and sodium methoxide (8.10 g, 0.150 mol) was added, and the reaction mixture was placed back under a hydrogen atmosphere and shaken for 18 h. The mixture was filtered through Celite to remove catalyst, and the solvent was removed to provide pure **12** as a white solid (74 g, 100%): mp 146–148 °C; <sup>1</sup>H NMR (DMSO, 300 MHz) δ 0.09 (s, 3H), 0.11 (s, 3H), 0.82 (s, 3H), 0.86 (s, 9H), 0.94 (s, 3H), 1.71 (m, 1H), 3.78 (t, 1H), 4.27 (m, 2H), 4.53 (d, 1H), 5.18 (s, 2H), 5.98 (d, 1H), 6.52 (d, 1H), 7.36 (m, 5H), 7.55 (d, 1H).

**2-[3-(Benzyloxycarbonyl)amino]-6-(3-hydroxyphenyl)-2-oxo-1,2-dihydro-1-pyridyl]-N-(3,3,3-trifluoro-1-isopropyl-2-oxopropyl)acetamide (10l).** To a solution of **10k** (78 mg, 0.13 mmol) in dry dichloromethane (3 mL) was added trifluoroacetic acid (0.08 mL, 1 mmol). After 18 h the reaction mixture was diluted with dichloromethane (50 mL), washed with water and brine, dried (MgSO<sub>4</sub>), and evaporated to a crude oil that was purified by chromatography (ethanol:ethyl acetate:dichloromethane, 0.5:5:94.5) to give **10l** as a white solid (60 mg, 85%); TLC *R<sub>f</sub>* = 0.15 (ethanol:ethyl acetate:dichloromethane, 0.5:5:94.5); <sup>1</sup>H NMR (DMSO/D<sub>2</sub>O, 300 MHz) δ 0.76 (d, 3H), 0.85 (d, 3H), 2.53 (m, 1H), 4.03 (d, 1H), 4.49 (m, 2H),

5.19 (s, 2H), 6.19 (d, 1H), 6.84 (m, 3H), 7.19 (t, 1H), 7.36 (m, 5H), 7.91 (d, 1H); MS (CI) *m/z* 546 (M + 1). Anal. (C<sub>27</sub>H<sub>26</sub>F<sub>3</sub>N<sub>3</sub>O<sub>6</sub>) C, H, N.

**2-[3-(Benzyloxycarbonyl)amino]-6-(4-carboxyphenyl)-2-oxo-1,2-dihydro-1-pyridyl]-N-(3,3,3-trifluoro-1-isopropyl-2-oxopropyl)acetamide (10p).** To a solution of **13** (96 mg, 0.16 mmol) in THF (0.7 mL) and water (0.14 mL) was added lithium hydroxide monohydrate (15.7 mg, 0.37 mmol) and the resulting solution allowed to stir for 3 h. The reaction mixture was diluted with water, and the pH was adjusted to 2 by addition of 10% hydrochloric acid. The product was extracted into ethyl acetate, and the organic extracts were then washed with brine. The solution was dried (MgSO<sub>4</sub>) and the solvent removed to give material that was recrystallized from hot ethyl acetate/hexane to provide pure **10p** (63 mg, 68%) as a white solid: TLC *R<sub>f</sub>* = 0.43 (ethanol:dichloromethane:acetic acid, 5:94.5:0.5); <sup>1</sup>H NMR (DMSO/D<sub>2</sub>O, 300 MHz) δ 0.77 (d, 3H), 0.87 (d, 3H), 2.24 (m, 1H), 4.07 (d, 1H), 4.44 (d, 1H), 4.68 (d, 1H), 5.22 (s, 2H), 6.29 (d, 1H), 7.35–7.53 (m, 8H), 8.01 (m, 2H); MS (CI) *m/z* 574 (M + 1). Anal. (C<sub>28</sub>H<sub>26</sub>F<sub>3</sub>N<sub>3</sub>O<sub>7</sub>) C, H, N.

**6-Phenethylpyrid-2-one-3-carbonitrile (19).** To a –78 °C solution of LDA (prepared from diisopropyl amine (6.6 mL, 47 mmol) and *n*-butyllithium (19 mL of a 2.14 M solution in hexane)) in THF (200 mL) was added a solution of **16** (2.5 g, 18.6 mmol) and the mixture allowed to warm to 0 °C. After stirring for 2 h, benzyl bromide (2.2 mL, 18.6 mmol) was added, and the solution was allowed to warm to room temperature and stir overnight. The solvents were evaporated, and the residue was taken up in water and washed with ether to remove unreacted benzyl bromide. The aqueous solution was made acidic to pH 3 with 1 N hydrochloric acid and the resulting precipitate collected and washed with water. The material was dried and chromatographed (methanol:chloroform, 3:97) to provide **19** (2.1 g, 50%) as a tan solid: <sup>1</sup>H NMR (DMSO, 300 MHz) δ 2.88 (m, 4H), 6.21 (d, 1H), 7.27 (m, 5H), 8.01 (d, 1H), 12.7 (bs, 1H); MS (CI) *m/z* 225 (M + 1).

**3-[3-(Benzyloxycarbonyl)amino]-6-phenethylpyrid-2-one (23).** A solution of **19** (2.15 g, 9.6 mmol) in 48% HBr (10 mL) and glacial acetic acid (20 mL) was heated at reflux for 12 h. The solution was cooled and diluted with water, and the pH was adjusted to 5 with 10% sodium hydroxide. The resulting precipitate was filtered and the solid washed with 10% hydrochloric acid and water. The solid was dried under vacuum to afford the carboxylic acid (2.1 g). The acid was dissolved in dioxane (40 mL), and to this was added triethylamine (1.1 mL, 8.25 mmol) and DPPA (1.8 mL, 8.36 mmol) followed by heating at reflux for 1 h. Benzyl alcohol (1.0 mL, 9.8 mmol) was added to the solution followed by refluxing for an additional 12 h. The solution was cooled and the solvent removed. The residue was dissolved in ethyl acetate, washed with 10% hydrochloric acid and brine, and dried (MgSO<sub>4</sub>), and the solvent was removed. The material was purified by chromatography (methanol:dichloromethane, 3:97) to provide pure **23** (1.71 g, 60%) as a cream-colored solid: <sup>1</sup>H NMR (DMSO, 300 MHz) δ 2.50 (m, 2H), 2.86 (m, 2H), 5.14 (s, 2H), 6.01 (d, 1H), 7.18–7.40 (m, 10H), 7.70 (d, 1H), 8.26 (s, 1H), 12.03 (s, 1H); MS (CI) *m/z* 349 (M + 1).

**3-[3-(Benzyloxycarbonyl)amino]-2-oxo-6-phenethyl-1,2-dihydro-1-pyridyl]acetic Acid (27).** Compound **23** (1.64 g, 4.7 mmol) was suspended in dry dimethylformamide (20 mL), and to this suspension was added NaH (0.22 g of a 60% mineral oil dispersion, 5.5 mmol). The mixture was stirred for 1.5 h, at which point all solids were in solution. *tert*-Butyl bromoacetate (0.92 g, 4.7 mmol) was added, and the mixture was stirred overnight. The mixture was diluted with water (100 mL) and extracted with ethyl acetate (four times). The extracts were washed with brine, dried (MgSO<sub>4</sub>), and evaporated. The residue was purified by chromatography (gradient elution, methanol:dichloromethane, 0:100 to 3:97) to give the *tert*-butyl ester (0.578 g, 27%). This material was dissolved in dichloromethane (10 mL), to this was added trifluoroacetic acid (1.5 mL), and the solution was allowed to stir for 12 h. The solvents were evaporated to afford pure **27** (0.48 mg, 98%): <sup>1</sup>H NMR (DMSO, 300 MHz) δ 2.85 (s, 4H), 4.66 (s, 2H),



5.15 (s, 2H), 6.16 (d, 1H), 7.19–7.43 (m, 10H), 7.77 (d, 1H), 8.39 (s, 1H); MS (CI)  $m/z$  407 (M + 1).

**2-[3-[(Benzyloxycarbonyl)amino]-2-oxo-6-phenethyl-1,2-dihydro-1-pyridyl]-N-(3,3,3-trifluoro-2-hydroxy-1-isopropylpropyl)acetamide (Step h, Scheme 4, R<sub>1</sub> = Phenethyl).** Compound **27** (0.50 g, 1.2 mmol) was dissolved in dry tetrahydrofuran (15 mL) along with 3-amino-1,1,1-trifluoro-4-methyl-2-pentanol hydrochloride (0.25 g, 1.2 mmol), EDC (0.23 g, 1.2 mmol), 4-methylmorpholine (0.27 g, 2.7 mmol), and 1-hydroxybenzotriazole hydrate (0.47 g, 3.5 mmol). The mixture was stirred for 2 days. The reaction mixture was evaporated and the residue partitioned between ethyl acetate (50 mL) and 10% hydrochloric acid (25 mL). The layers were separated, and the organic solutions were washed with 10% hydrochloric acid, saturated sodium bicarbonate, and brine, dried (MgSO<sub>4</sub>), and evaporated to a foam. The material was purified by chromatography (methanol:dichloromethane, 4:96) to provide the alcohol (0.51 g, 76%): TLC  $R_f$  = 0.48 (methanol:dichloromethane, 4:96); <sup>1</sup>H NMR (DMSO, 300 MHz)  $\delta$  0.81 (d, 3H), 0.89 (d, 3H), 1.80 (m, 1H), 2.72 (m, 2H), 2.84 (m, 2H), 3.79 (t, 1H), 4.11 (m, 1H), 4.88 (m, 2H), 5.15 (s, 2H), 6.12 (d, 1H), 6.54 (d, 1H), 7.15–7.43 (m, 10H), 7.76 (d, 1H), 8.04 (d, 1H), 8.33 (s, 1H); MS (CI)  $m/z$  560 (M + 1).

**3-Cyano-4-phenylpyrid-2-one (28).** Toluene (200 mL) was added to a mixture of acetophenone (24.1 g, 200 mmol), cyanoacetamide (16.8 g, 200 mmol), ammonium acetate (15.4 g, 200 mmol), and acetic acid (34.4 mL, 600 mmol), and the resulting homogeneous solution was heated at reflux for 18 h. After cooling to ambient temperature, the precipitated solid was filtered and washed with toluene to afford 18.2 g of crude material. Recrystallization from ethanol afforded 2-cyano-3-phenylbutyramide (7.75 g, 21%) as a yellow solid: <sup>1</sup>H NMR (DMSO, 300 MHz)  $\delta$  2.35 (s, 3H), 7.49 (m, 5H), 7.82 (brs, 1H), 8.07 (brs, 1H); MS (CI)  $m/z$  187 (M + 1).

A solution of this material and dimethylformamide diethyl acetal (6.44 g, 43.7 mmol) in DMF (14 mL) was heated at reflux for 6 h, during which time liberated ethanol was removed by distillation. Excess DMF was then removed on a rotary evaporator (<1 Torr of pressure). After standing for 18 h the resulting solid was slurried in methanol and the solid isolated by filtration to afford **28** (3.3 g, 40%) as a white solid: <sup>1</sup>H NMR (DMSO, 250 MHz)  $\delta$  6.44 (d, 1H), 7.60 (m, 5H), 7.82 (d, 1H), 12.62 (brs, 1H); MS (CI)  $m/z$  197 (M + 1).

**2-[3-[(Benzyloxycarbonyl)amino]-2-oxo-5-phenyl-1,2-dihydro-1-pyridyl]-N-(3,3,3-trifluoro-2-hydroxy-1-isopropylpropyl)acetamide (Steps d and e, Scheme 5).** To a solution of **30** (2.65 g, 3.81 mmol) in THF (20 mL) was added tetrakis(triphenylphosphine)palladium(0) (1.0 g, 0.87 mmol) and the solution stirred for 0.5 h. A solution of phenylboric acid (0.92 g, 7.62 mmol) in ethanol (20 mL) was added followed by stirring for 1 h. A solution of sodium carbonate (20 mL of a 2 M solution in water) was then added, and the reaction was refluxed for 3 h. The product was extracted into ether, washed with water, and dried (MgSO<sub>4</sub>). The solvents were evaporated and then redissolved in THF (50 mL), and to this was added a solution of tetrabutylammonium fluoride (5 mL of a 1 M solution in THF) followed by stirring for 5 min. The reaction was diluted with ethyl acetate and washed with saturated ammonium chloride, water, and brine. The solution was dried (MgSO<sub>4</sub>), and the solvent was removed. The resulting material was purified by chromatography (methanol:dichloromethane, 5:95) to provide the title compound (1.36 g, 67%) as an off-white solid: mp 202–204 °C; <sup>1</sup>H NMR (DMSO, 300 MHz)  $\delta$  0.89–0.93 (m, 6H), 1.81 (m, 1H), 3.85 (t, 1H), 4.13 (m, 1H), 4.64 (d, 1H), 4.84 (d, 1H), 5.19 (s, 2H), 6.55 (d, 1H), 7.30–7.52 (m, 10H), 7.73 (d, 1H), 8.06 (d, 1H), 8.22 (d, 1H), 8.55 (s, 1H). Anal. (C<sub>27</sub>H<sub>28</sub>F<sub>3</sub>N<sub>3</sub>O<sub>5</sub>) C, H, N.

**Molecular Modeling.** Molecular mechanics (MM) computations were performed *in vacuo*, using the AESOP force field<sup>34</sup> and the in-house graphics program ENIGMA.<sup>35</sup> Only those residues within 12 Å of the active site region of the HLE–TOMI X-ray crystal structure were included in these computations. HLE atoms were constrained to their position in the X-ray structure for these computations.

Molecular dynamics (MD) and free energy perturbation (FEP) simulations<sup>36</sup> were performed using the program

AMBER3.0a<sup>37</sup> and the united atom model. The starting geometry for HLE was taken from the X-ray molecular structure of the HLE–TOMI complex.<sup>16</sup> The noncovalently bound TOMI fragment was removed, as were the HLE-bound sugars, which are remote from the active site. Inhibitors were covalently attached via the (trifluoromethyl)carbonyl carbon to Ser-195 as the oxyanion. The inhibitors were initially docked into the active site in a manner analogous to the arrangement observed for peptidic inhibitors in PPE.<sup>17</sup> The selection of this binding motif has been further supported by subsequent X-ray crystallographic analysis of selected pyridone-based inhibitors in PPE.<sup>38</sup> Atomic partial charges were obtained for the pyridone fragments of the inhibitors via electrostatic potential energy surface (EPS) fit using the program CHELPG<sup>39</sup> to 6-31G\*\*/6-31G\* *ab initio* wave functions Gaussian 88. EPS derived 6-31G\*\*/6-31G\* charges were also employed for the (trifluoromethyl)alkoxide portion of the inhibitor. United atom AMBER3.0a charges for valine were used for the P<sub>1</sub> portion of the inhibitor and the 6-position phenyl. All atomic charges for the inhibitors investigated in this work are reported in the supplementary material.<sup>40</sup>

A 20 Å cap of TIP3P water with a weak restoring force<sup>39</sup> was placed over the active site of the enzyme–inhibitor complex. This resulted in the addition of approximately 450 water molecules to the computations. Previous comparisons of trajectories obtained for HLE bound inhibitors under aqueous periodic boundary conditions suggest that the described water-cap conditions are a reasonable approximation for the active site region of this enzyme.<sup>35</sup>

Initial structures were minimized for 250 cycles of steepest decent optimization prior to beginning dynamics. MD was initiated at 10 K and equilibrated to 298 K using an 8.0 Å cutoff radius. A time step of 0.001 ps was employed throughout the simulation and data was collected every 0.1 ps. A pair list update was performed every 0.02 ps. Simulations for each inhibitor or enzyme–inhibitor complex were performed over 50 ps, using the final 40 ps for analysis. Equilibrated (50 ps) end points from MD simulations were used as starting structures for FEP.

FEP simulations were performed using coordinate decoupling with 51 windows of 0.5 ps equilibration followed by 0.5 ps data collection employed for electrostatic modifications followed by 51 ps of slow growth for the nonbonded component for a total of 102 ps. These simulation times compare well and/or are longer than those used successfully in previous studies.<sup>41</sup> FEP simulations were performed using periodic boundary conditions for isolated inhibitors (i.e.,  $\Delta\Delta G$  for [10f → 10a]<sub>aq</sub>) and a 20 Å water cap (above) over the active site region when inhibitors were docked in HLE (i.e.,  $\Delta\Delta G$  for [HLE-10f → HLE-10a]<sub>aq</sub>). Selected perturbations were tested for equilibration by explicit reverse perturbation. In addition, all hysteresis values were found to be within acceptable ranges.

Throughout our inhibitor design efforts, molecular graphics and *in vacuo* molecular mechanics computations were used initially to determine whether potential inhibitors had geometric features that reasonably allowed for the formation of the desired interactions with HLE. Aqueous MD simulations were then employed to test whether such interactions could be expected under conditions that more accurately represent the experimental environment.

**Acknowledgment.** The authors wish to thank Drs. Andrew Shaw, Fred Brown, Peter Bernstein, Brian Masek, and Roy Thomas for helpful suggestions throughout the course of this work and in preparation of the manuscript.

**Supplementary Material Available:** Atom-centered charges for molecular dynamics and free energy perturbation simulations are given for compound **10f** (1 page). Ordering information is given on any current masthead page.

## References

- (1) For recent reviews, see: (a) Bode, W.; Meyer, E., Jr.; Powers, J. C. Human Leukocyte and Porcine Pancreatic Elastase: X-ray Crystal Structures, Mechanism, Substrate Specificity, and Mecha-

- nism-Based Inhibitors. *Biochemistry*, **1989**, *28*, 1951–1963. (b) Weinbaum, G.; Giles, R. E.; Krell, R. D., Eds. Pulmonary Emphysema. *N. Y. Acad. Sci.* **1991**, *624*, 1–370. (c) Edwards, P. D.; Bernstein, P. R. Synthetic Inhibitors of Elastase. *Med. Res. Rev.* **1994**, *14*, 127–194.
- (2) Hubbard, R. C.; Brantly, M. L.; Sellers, S. E.; Mitchell, M. E.; Crystal, R. G. Anti-Neutrophil-Elastase Defenses of the Lower Respiratory Tract in  $\alpha$ 1-Antitrypsin Deficiency Directly Augmented with an Aerosol of  $\alpha$ 1-Antitrypsin. *Ann. Intern. Med.* **1989**, *111*, 206–212.
  - (3) Thompson, R. C.; Ohlsson, K. Isolation, Properties, and Complete Amino Acid Sequence of Secretory Leukocyte Protease Inhibitor, a Potent Inhibitor of Leukocyte Elastase. *Proc. Natl. Acad. Sci. U.S.A.* **1986**, *83*, 6692–6696.
  - (4) Wiedow, O.; Schroder, J.-M.; Gregory, H.; Young, J. A.; Christophers, E. Elafin: An Elastase-specific Inhibitor of Human Skin. *J. Biol. Chem.* **1990**, *265*, 14791–14795.
  - (5) Sallenave, J.-M.; Marsden, M. D.; Ryle, A. P. Isolation of Elafin an Elastase-Specific Inhibitor (ESI) from Bronchial Secretions. *Biol. Chem. Hoppe-Seyler* **1992**, *373*, 27–33.
  - (6) Eriksson, S. The Potential Role of Elastase Inhibitors in Emphysema Treatment. *Eur. Respir. J.* **1991**, *4*, 1041–1043.
  - (7) Nadel, J. Role of Mast Cell and Neutrophil Proteases in Airway Secretion. *Am. Rev. Respir. Dis.* **1991**, *144*, S48–S51.
  - (8) Jackson, A. H.; Hill, S. L.; Afford, S. C.; Stockley, R. A. Sputum Soluble Phase Proteins and Elastase Activity in Patients with Cystic Fibrosis. *J. Respir. Dis.* **1984**, *65*, 114–124.
  - (9) Tosi, M. F.; Zakem, H.; Berger, M. Neutrophil Elastase Cleaves C3bi on Opsonized Pseudomonas as well as CR1 on Neutrophils to Create a Functionally Important Opsonin Receptor Mismatch. *J. Clin. Invest.* **1990**, *86*, 300–308.
  - (10) Bergeson, S.; Schwartz, J. A.; Stein, M. M.; Wildonger, R. A.; Edwards, P. D.; Shaw, A.; Trainor, D. A.; Wolanin, D. J. U.S. Patent 4,910,190, 1990; *Chem. Abstr.* **1991**, *114*, 123085m.
  - (11) Stein, M. M.; Wildonger, R. A.; Trainor, D. A.; Edwards, P. D.; Yee, Y. K.; Lewis, J. J.; Zottola, M. A.; Williams, J. C.; Strimpler, A. M. In Vitro and In Vivo Inhibition of Human Leukocyte Elastase (HLE) by Two Series of Electrophilic Carbonyl Containing Peptides. *Peptides: Chemistry, Structure, and Biology (Proceedings of the Eleventh American Peptide Symposium)*; Rivier, J. E., Marshall, G. R., Eds.; ESCOM Science: Leiden, 1990; pp 369–370.
  - (12) Williams, J. C.; Falcone, R. C.; Kneec, C.; Stein, R. L.; Strimpler, A. M.; Reaves, B.; Giles, R. E.; Krell, R. D. Biologic Characterization of ICI-200,880 and ICI-200,355 Novel Inhibitors of Human Neutrophil Elastase. *Am. Rev. Respir. Dis.* **1991**, *144*, 875–883.
  - (13) (a) Brown, F. J.; Andisik, D. W.; Bernstein, P. B.; Bryant, C. B.; Ceccarelli, C.; Damewood, J. R., Jr.; Edwards, P. D.; Earley, R. A.; Feeney, S.; Green, R. C.; Gomes, B. C.; Kosmider, B. J.; Krell, R. D.; Shaw, A.; Steelman, G. B.; Thomas, R. M.; Vacek, E. P.; Veale, C. A.; Tuthill, P. A.; Warner, P.; Williams, J. C.; Wolanin, D. J.; Woolson, S. A. The Design of Orally Active, Nonpeptidic Inhibitors of Human Leukocyte Elastase. *J. Med. Chem.* **1994**, *37*, 1259–1261. (b) Warner, P.; Green, R. C.; Gomes, B. C.; Williams, J. C. Nonpeptidic Inhibitors of Human Leukocyte Elastase. 1. The Design and Synthesis of Pyridone-Containing Inhibitors. *J. Med. Chem.* (accepted for publication).
  - (14) Bernstein, P. B.; Andisik, D.; Bradley, P.; Bryant, C.; Ceccarelli, C.; Damewood, J. R.; Earley, R.; Feeney, S.; Gomes, B.; Kosmider, B. J.; Steelman, G. B.; Thomas, R. M.; Vacek, E. P.; Veale, C. A.; Williams, J. C.; Wolanin, D. J.; Woolson, S. A. Nonpeptidic Inhibitors of Human Leukocyte Elastase. 3. Design, Synthesis, X-ray Crystallographic Analysis, and Structure-Activity Relationships for a Series of Orally Active 3-Amino-6-phenyl-2-oxopyridinyl Trifluoromethyl Ketones. *J. Med. Chem.*, following paper in this issue.
  - (15) Veale, C. A.; Bernstein, P. R.; Bryant, C.; Ceccarelli, C.; Damewood, J. R. Jr.; Earley, R.; Gomes, B.; Kosmider, B. J.; Steelman, G. B.; Thomas, R. M.; Vacek, E. P.; Williams, J. C.; Woolson, S. A. Nonpeptidic Inhibitors of Human Leukocyte Elastase. 5. Design, Synthesis, Structure-Activity Relationships, and X-Ray Crystallography of a Series of Orally Active 5-amino-2-arylpiperidinones. *J. Med. Chem.* In press.
  - (16) Bode, W.; Wei, A. Z.; Huber, R.; Meyer, E.; Travis, J.; Neumann, S. X-Ray Crystal Structure of the Complex of Human Leukocyte Elastase (PMN Elastase) and the Third Domain of the Turkey Ovomucoid Inhibitor. *EMBO J.* **1986**, *5*, 2453–2458.
  - (17) Takahashi, L. H.; Radhakrishana, R.; Rosenfield, R. E.; Meyer, E. F., Jr.; Trainor, D. A.; Stein, M. X-Ray Diffraction Analysis of the Inhibition of Porcine Pancreatic Elastase by a Peptidyl Trifluoromethylketone. *J. Mol. Biol.* **1988**, *210*, 423–428.
  - (18) Takahashi, L. H.; Radhakrishana, R.; Rosenfield, R. E., Jr.; Meyer, E. F., Jr.; Trainor, D. A. Crystal Structure of the Covalent Complex Formed by a Peptidyl  $\alpha, \alpha$ -Difluoro- $\beta$ -keto Amide with Porcine Pancreatic Elastase at 1.78-Å Resolution. *J. Am. Chem. Soc.* **1989**, *111*, 3368–3373.
  - (19) Edwards, P. D.; Meyer, E. F., Jr.; Vijayalakshmi, J.; Tuthill, P. A.; Gomes, B. C.; Strimpler, A. Design, Synthesis, and Kinetic Evaluation of a Unique Class of Elastase Inhibitors, the Peptidyl  $\alpha$ -Ketobenzoxazoles, and the X-Ray Crystal Structure of the Covalent Complex between Porcine Pancreatic Elastase and Ac-Ala-Pro-Val-2-Benzoxazole. *J. Am. Chem. Soc.* **1992**, *114*, 1854–1863.
  - (20) Edwards, P. D.; Hesp, B.; Trainor, D. A.; Willard, A. K. Enzymes as Targets for Drug Design. In *Enzyme Chemistry: Impact and Applications*, 2nd ed.; Suckling, C. J., Ed. Chapman and Hall: London, 1990; pp 207–218.
  - (21) Wolanin, D. J. Unpublished observations.
  - (22) Robertson, D. W.; Beedle, E. E.; Swartzendruber, J. K.; Jones, N. D.; Elzey, T. K.; Kauffman, R. F.; Wilson, H.; Hayes, J. S. Bipyridine Cardiotonics: The Three-Dimensional Structures of Amrinone and Milrinone. *J. Med. Chem.* **1986**, *29*, 635–640.
  - (23) Sircar, I.; Duell, B. L.; Bristol, J. A.; Weishaar, R. E.; Evans, D. B. Cardiotonic Agents. 5. 1,2-Dihydro-5-[4-(1H-imidazol-1-yl)-phenyl]-6-methyl-2-oxo-3-pyridinecarbonitriles and Related Compounds. Synthesis and Inotropic Activity. *J. Med. Chem.* **1987**, *30*, 1023–1029.
  - (24) Ninomiya, K.; Shioiri, T.; Yamada, S. Amino Acids and Peptides XII. *Chem. Pharm. Bull.* **1974**, *22*, 1398–1404.
  - (25) Bernstein, P. R.; Shaw, A.; Thomas, R. M.; Warner, P.; Wolanin, D. J. Heterocyclic Amides Having HLE Inhibiting Activity. European Patent Application 509,769 A2, published October 21, 1992.
  - (26) The structure activity relationships of pyridones containing substitution on the 3-amino group is the subject of the following paper in this series.
  - (27) Fearon, K.; Spaltenstein, A.; Hopkins, P. B.; Gelb, M. H. Fluoro Ketone Containing Peptides as Inhibitors of Human Renin. *J. Med. Chem.* **1987**, *30*, 1617–1622.
  - (28) Mariella, R. P. *Organic Synthesis*; Rabiohn, N., Ed.; John Wiley and Sons, Inc.: New York, 1963; Collect. Vol. IV, p 210.
  - (29) DeJohn, D.; Domagala, J. M.; Kaltenbronn, J. S.; Krolls, U. Functionalization of Substituted 2(1H)- and 4(1H)-Pyridones. III. *J. Heterocycl. Chem.* **1983**, *20*, 1295–1302.
  - (30) Iihama, T.; Fu, J.-M.; Bourguignon, M.; Snieckus, V. Regiospecific Syntheses of All Isomeric Nitrofluorenes and Nitrofluorenes by Transition Metal Catalyzed Cross-Coupling Reactions. *Synthesis* **1989**, 184–187.
  - (31) The calculated log *P*'s for these compounds are **10f** = 5.1; **31** = 5.1; and **29** = 4.9. Calculated using CLOGP3 v3.4, MedChem Software, Daylight Chemical Information Systems, 2 Corporate Park, Suite 204, Irvine CA 92714.
  - (32) Molecular dynamics simulations have also been performed for a related enzyme, porcine pancreatic elastase (PPE). For example, see: Geller, M.; Swanson, W. M.; Meyer, E. F., Jr. Dynamic Properties of the First Steps of the Enzymatic Reaction of Porcine Pancreatic Elastase (PPE). 2. Molecular Dynamics Simulation of a Michaelis Complex: PPE and the Hexapeptide Thr-Pro-Nal-Leu-Tyr-Thr. *J. Am. Chem. Soc.* **1990**, *112*, 8925–8931 and references therein.
  - (33) Work in a related series of inhibitors has shown that a 6-position isopropyl or cyclohexyl-group were both inferior in *K<sub>i</sub>* to phenyl substitution. This work will be described in a future paper in this series. Attempts to incorporate a 6-*tert*-butyl group into these molecules failed due to extensive O-alkylation of the pyridone ring with iodide 7.
  - (34) AESOP is an in-house molecular mechanics program (Masek, B. Zeneca, Inc., 1800 Concord Pike, Wilmington, DE 19897) derived from BIGSTRN-3 (QCPE 514): Nachbar, R., Jr.; Mislow, K. *QCPE Bull.* **1986**, *6*, 96. AESOP employs the MM2 force field.
  - (35) ENIGMA is an in-house molecular graphics program: Zeneca, Inc., 1800 Concord Pike, Wilmington, DE 19897.
  - (36) For reviews of the molecular dynamics method, see: McCammon, J. A.; Harvey, S. C. *Dynamics of Proteins and Nucleic Acids*; Cambridge University Press: New York, 1987. Brooks, C. L. III; Karplus, M.; Pettitt, B. M. *Proteins. A Theoretical Perspective of Dynamics, Structure and Thermodynamics*; John Wiley & Sons: New York, 1988. van Gunsteren, W. F.; Weiner, P. K. *Computer Simulation of Biomolecular Systems. Theoretical and Experimental Applications*; Escom: Leiden, 1989.
  - (37) Singh, U. C.; Weiner, P.; Caldwell, J. C.; Kollman, P. A. (1989), AMBER 3.0 Revision A., University of California, San Francisco.
  - (38) Ceccarelli, C. Personal communication.
  - (39) Determining atom-centered monopoles from molecular electrostatic potentials: Brenneman, C. M.; Wiberg, K. B. The Need for High Sampling Density in Formamide Conformational Analysis. *J. Comput. Chem.* **1990**, *11*, 361–373. We thank C. M. B. for sharing his modified version of CHELP with us.
  - (40) Gaussian 88, Revision C Version (1988), Gaussian, Inc. 4415 Fifth Avenue, Pittsburgh, PA 15213.
  - (41) For example, see: Caldwell, J. W.; Agard, D. A.; Kollman, P. A. Free Energy Calculations on Binding and Catalysis by  $\alpha$ -Lytic Protease: The role of Substrate Size in the P<sub>1</sub> Pocket. *Proteins: Struct. Funct. Genetics* **1991**, *10*, 140–148.